

Predicting small-scale fading distributions with Finite-Difference methods in Indoor-to-Outdoor scenarios

Alvaro Valcarce, David López-Pérez, Guillaume De La Roche, Jie Zhang
Centre for Wireless Network Design (CWIND)
University of Bedfordshire, Luton, Bedfordshire, UK
alvaro.valcarce@beds.ac.uk

Abstract—Finite-Difference electromagnetic methods have been used for the deterministic prediction of radio coverage in cellular networks. This paper introduces an approach that exploits the spatial power distribution obtained from these techniques to characterize the random variations of fading due to multipath propagation. Although the presented method is equally applicable to any Finite-Difference algorithm able of computing electromagnetic field patterns (e.g. PSTD, ParFlow, ...), it has been exemplified here by means of FDTD. Furthermore, in order to test the reliability of this approach, the predicted fading distributions are compared against real measurements in a residential Indoor-to-Outdoor scenario. Finally, the practical usability of this fading prediction approach is tested throughout implementation in a WiMAX femtocells system-level simulator.

I. INTRODUCTION

The need for radio network planning tools that aid operators to design and optimize their wireless infrastructure is rising. In order to increase the reliability of these tools, accurate radio wave propagation models are necessary. But it is important to notice that the knowledge of the received signal level is not sufficient to evaluate correctly the performance of a system. Random small-scale fading creates changes in the received signal amplitude, that can have a profound impact on the quality of the reception, as well as on the global performance.

Propagation prediction methods have been traditionally used to describe either indoor or outdoor environments. However nowadays, with nearly 60% of phone calls taking place indoors [1], and the advent of technologies such as femtocells or indoor-located macrocells and handsets, the study of the indoor-to-outdoor propagation conditions is more necessary than ever.

In this paper, the aim is first to use a deterministic propagation model, to provide a coverage map of the received signal at a very fine resolution. Then, in a second step, the distribution of the received signal can be analyzed to extract fading parameters that can be taken into account by a system-level simulation tool.

In section II, the FDTD model implementation based on a measurements-based calibration is presented. Then in section III an indoor-to-outdoor fading model will be extracted from the FDTD propagation prediction, and matched against a measured fading distribution. Finally, section IV presents the inclusion of the indoor-to-outdoor fading model in a system-

level tool to study the potential performance of a real system. As an example of the applicability of an indoor-to-outdoor fading model, the used scenario was that of a WiMAX femtocell hybrid network. To conclude, the advantages of using this approach for the prediction of fading will be summarized.

II. THE FDTD PROPAGATION MODEL

The Finite-Difference Time-Domain [2], is a method that approximates the solution to the Maxwell equations by means of a discretization in the spatial and time domains. It is therefore a suitable way of performing electromagnetic simulations and it has been already widely applied in the industry, specially in the design of antennas and microwave circuits.

However, the high computational load of the FDTD algorithm has kept it back from being applied to the finding of solutions in larger scenarios such as suburban or urban areas. In order to circumvent this barrier, in [3] a 2D implementation of FDTD has been proposed. This approach exploits the different memory addressing modes of modern graphics cards along with their parallel computing capacity, reaching processing speeds of around 800 Mcps¹ on one PC equipped with a high-performance GPU card. Such implementation is used in this paper as a fast way for predicting electromagnetic indoor-to-outdoor propagation. In addition, FDTD is equally formulated for indoor and outdoor scenarios, being hence very suitable for hybrid indoor-to-outdoor propagation predictions such as in the case of femto-to-macro interference.

An FDTD coverage simulation by itself represents however nothing but a theoretical prediction of what the propagation environment potentially looks like. In order to verify such a prediction, it is thus necessary to match it against real channel measurements. This way, an estimation of the error of the simulation can be obtained for comparison and verification with other propagation models.

For this work, a measurements campaign of the indoor-to-outdoor channel path loss has therefore been performed. The transmitter² was located inside of a house in a residential area of Luton (a town in the north of London, U.K.), while the

¹Megacells per second

²A vector signal generator *MG3700A* from *Anritsu* has been used for the generation of the radiated signal.

TABLE I
TUNED MATERIALS PARAMETERS AT $(f_{real}, f_{sim}) = (3.5, 0.25)GHz$

	ϵ_r	μ_r	σ
Air	1.8824	0.7280	$7.2273 \cdot 10^{-4}$
Plaster	1.1182	1.2779	0.0196
Wood	1.7522	0.2802	0.0440
Glass	5.1358	1.2516	0.0045
Brick	3.5789	7.661	0.0014

received power was recorded in the street adjacent to the house hosting the transmitter. The generated signal was an oscillatory pulse at the frequency of $f = 3.5GHz$ and the radiated RMS power was $3dBm$. By applying optimization algorithms such as metaheuristics, it is possible [4] to perform a search for the combination of materials parameters that produces the highest resemblance between simulation and measurements results. For this study, a search based on Simulated Annealing [5] has been applied. This yields as final solution, the configuration of materials shown in Table I, where ϵ_r represents the relative electrical permittivity, μ_r the relative magnetic permeability and σ the electrical conductivity (in $S \cdot m^{-1}$) of the different materials involved in the simulation.

For efficiency reasons, the FDTD simulation frequency f_{sim} is typically different from the system's real frequency f_{real} (see [6] for details) and hence the calibrated parameters will vary at different f_{sim} . For the parameters shown in Table I, the simulation frequency was $f_{sim} = 250MHz$. With respect to the accuracy of this model, the error between the FDTD prediction and the measurements is $RMSE = 6dB$, which compares well with other propagation models.

III. INDOOR-TO-OUTDOOR FADING MODEL

As explained in the introduction, the main purpose of this work was to create a reliable fading model, suitable for its implementation on a system-level simulator (SLS) for WiMAX femtocells. By making use of an efficient GPU implementation, it is reasonable to make use of the FDTD algorithm for the calculation of accurate coverage predictions within low computing times during system-level simulations. This paper extends thus the usefulness of FDTD from coverage prediction in SLS to the prediction of scenario-dependant localized fading distributions.

A. Fading extracted from FDTD predictions

The method proposed here for the extraction of fading statistics at different locations in the simulation scenario, consists on performing a local analysis of the power distribution of the predicted field pattern.

Following an approach similar to [7] and for any given location in the simulation scenario, a fading region FR_p of radius R_p is extracted from an area surrounding the analysis point p . In Figure 1, for instance, field patterns corresponding to fading regions around two sample random locations of the simulated scenario are presented.

In [7], the authors used square areas around p , which has the disadvantage of not keeping a constant proportion of fading

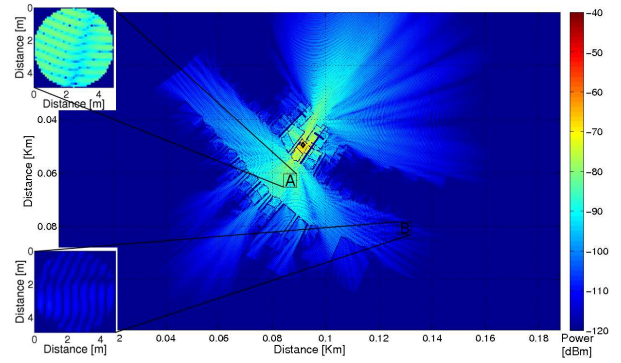


Fig. 1. Extraction of fading regions of radius $4\lambda_{sim}$ from a femtocell coverage prediction obtained with a WiMAX-frequency-calibrated FDTD model.

points that are at the same distance from the point of interest. To solve this issue, the approach presented here uses circular regions in order to guarantee that equally distant locations have the same weight in the final distribution.

Ideally and in order to guarantee that the channel behavior remains approximately constant in the fading region, R_p should be approximately equal to the coherence distance D_c , which is a function of the angular spread of the received multipath components [8]. Since estimating the angle of arrival (AOA) of multipath components is out of the scope of this paper, a simplification has been applied here by choosing a fading region of size $R_{FR} = 4\lambda_{sim}$, being λ_{sim} the wavelength at the simulation frequency³.

Since open spaces in households suffer a delay spread on the order of $\tau_{rms} \approx 16ns$ [9], it is possible to use the distance d_τ that the signal travels in a period of τ_{rms} as an approximation to the coherence distance. Therefore, $D_c \approx \tau_{rms} \cdot c$, where c is the speed of light. The simulation frequency used for this study was $f_{sim} = 250MHz$ so it is easy to see that,

$$D_c \approx \tau_{rms} \cdot c = \tau_{rms} \cdot \lambda_{sim} \cdot f_{sim} |_{\tau \approx 16ns} \approx 4 \cdot \lambda_{sim} \quad (1)$$

Another equivalent approach would be to obtain the angle of arrival at the analysis point and extract the equivalent coherence distance.

The main advantage of using FDTD for the prediction of fading distributions is that it allows for the computation of localized fading distributions, i.e. the fading distribution will vary from point to point. This is made much clearer in Figure 2, where the fading histograms of the selected points are plotted. It is here possible to see how two distant regions are subject to different fading distributions. For example, point A in Figure 1 is located very close to the indoor transmitter and suffers fading according to a lognormal distribution. On the other hand, point B still receives a strong component from the direction of the transmitter plus several reflections from the other houses. This situation produces fading with a Rician distribution, much different from the previous case.

³Please note that, as detailed in [6], the FDTD simulation frequency f_{sim} and the real system's frequency f_{real} are not necessarily equal.

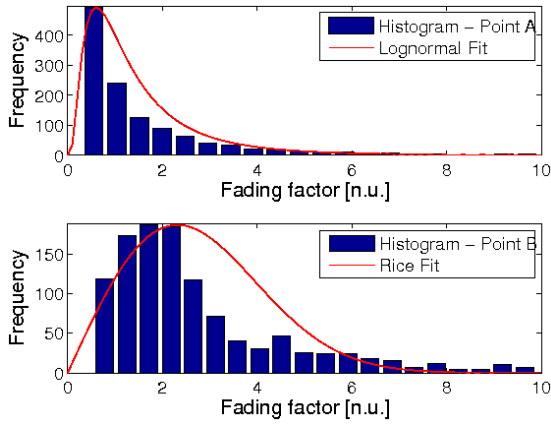


Fig. 2. Fading distributions of the regions extracted in Figure 1.

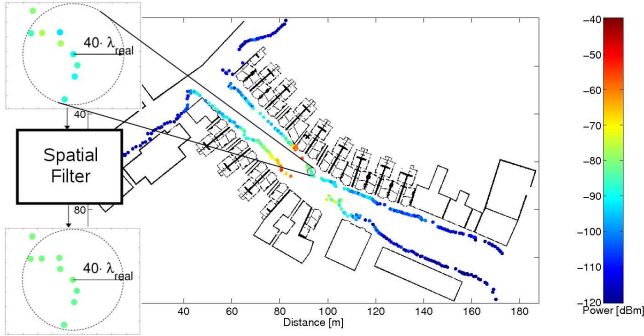


Fig. 3. Power measurements with fading laid over the simulation scenario. The *Spatial Filter* is centered at each measurement point and it removes fading by computing the mean power of the measurements that fall inside of its spatial domain.

Each fading region FR_p contains a large number of power values P_p that are subject to fading. These values are then compared to the predicted power P_p^{pred} at the point p under consideration so that their variation around P_p^{pred} can be accounted as realizations of the random variable that models fading at such location. If P_p^{pred} and P_p are expressed in dBm, the fading factor F_p at each location in the fading region is thus obtained by

$$F_p = P_p - P_p^{pred} \quad (2)$$

which is expressed in natural units by $f_p = 10^{F_p/10}$. Out of the different values of the fading factor computed from the fading region, it is then easy to apply Maximum Likelihood (ML) algorithms to fit f_p to a reasonable distribution. Figure 2 also illustrates this by displaying the calculated fits of the data extracted from the fading regions of Figure 1.

B. Fading extracted from measurements

In order to assess the reliability of the presented fading prediction model, a measurements campaign for the case of indoor-to-outdoor propagation has been carried out.

The raw power measurements are shown in Figure 3. In order to distinguish the power variations due to fading from

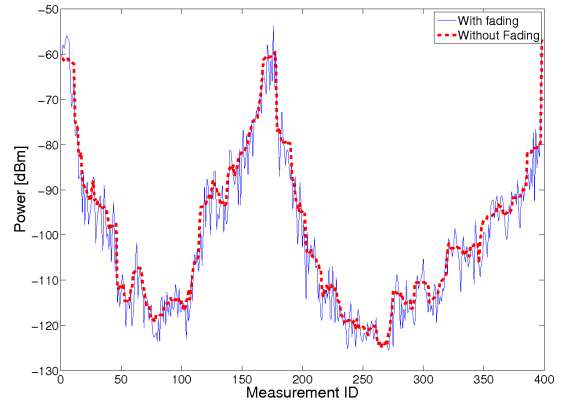


Fig. 4. Power measurements with fading (before spatial filtering) and without fading (after spatial filtering).

those caused by other propagation mechanisms, the small-scale fading must be removed from the measurements. This is achieved by means of a *Spatial Filter* (see Figure 3), which is a technique [10] used for the smoothing of data distributed over a 2D scenario. Following the *40 Lambda Averaging Criteria* [11] for the removal of small-scale fading, the window size for this filter is $40 \cdot \lambda_{real}$, being λ_{real} the wavelength at the frequency of the power measurements. The fading-removal effect of applying this filter is made evident in Figure 4, where the fadingless data is shown in comparison with the original values.

The obtained measurements must undergo an outliers-removal phase before they can actually be used for analysis. This includes mainly the removal of points subject to location⁴ errors and noise-bins (points with too low power values). After the removal of all the outliers, a total of $N = 398$ measurement points were available. Given the reduced size of the scenario, this is assumed to be enough for the extraction of fading statistics in the indoor-to-outdoor case.

In order to estimate the fading distribution of the measurements, the variation of the original data over the fadingless power values is computed in a similar way to the method used for the FDTD predictions. The fading factor F_p at the measurement point p , expressed in dBs is thus,

$$F_p = P_p^{unfiltered} - P_p^{filtered} \quad (3)$$

being $P_p^{unfiltered}$ the original power value before the spatial filtering is applied (and therefore subject to small-scale fading) and $P_p^{filtered}$ the power value after the removal of the fading effects by means of the spatial filter. The correlation coefficient between the measurements fading factor F_p and the FDTD model prediction error E has also been quantized by means of the Pearson product-moment coefficient [12], reaching a value of $\rho_{F_p, E} \approx 0.12$, which indicates a low degree of linear dependence between them both. It can be thus assumed that the deterministic model predictions are independent from the fading amplitude.

⁴The geolocalization of the measurement points was performed using a GPS receiver, which is obviously subject to reception errors.

TABLE II
COMPUTED FADING PARAMETERS FOR $R \sim Rice(\sigma, \nu)$

	$E(R)$	$Var(R)$	σ	ν	K factor
Prediction	1.031	0.2907	0.8229	0.000123	5.56
Measurements	1.194	0.3896	0.9528	0.00012	4.58

C. Comparison of the Fading Distributions

In order to compare the FDTD fading predictions with the measurements-based fading distribution, $N = 398$ fading regions have been extracted from the FDTD coverage prediction at the N exact locations of the measurement points. Since only N measurements-based fading values were available for the full scenario, the simulation scenario is in this case, treated as a whole for the extraction of the fading distribution. This means that, in order to compare the predictions with the measurements, the fading factors of all the fading regions extracted from the coverage prediction account to the general fading distribution of the global scenario. However, as explained in section III-A and illustrated in Figure 1, localized fading predictions are also possible.

By applying an ML estimation algorithm [13] to the fading factors obtained from the measurements and FDTD predictions, it has been found that, over the global scenario, the small-scale fading follows a Rician distribution. The parameters of such a distribution have been obtained throughout ML estimation and displayed in Table II.

A receiver located in the proximities (adjacent street) of a house containing a transmitter, will receive a strong signal component from the direction of the transmitter premises. Furthermore, it will receive lower power components from reflections, diffractions and other scatterers along the street. These multipath components add up all together with different phases producing small-scale fading effects. It has already been proven [14] that the power amplitude associated with this type of scenario follows a Rician distribution $Rice(\sigma, \nu)$, matching the FDTD-predicted distribution and increasing the validity of the presented method.

The Rician K factor is defined as the ratio of the power in the main signal component over the mean multipath received power and it is useful to measure the strength of the fading. It has been shown [15] that the K factor of a received signal R following a Rician fading distribution can be also computed empirically as:

$$K = \frac{\sqrt{1 - \frac{Var(R)}{E(R)}}}{1 - \sqrt{1 - \frac{Var(R)}{E(R)}}} \quad (4)$$

The computed K factors for the obtained distributions are thus also shown in Table II for comparative purposes. Similarly, the computed fading distributions for the global scenario are graphically presented in Figure 5, where the Cumulative Distribution Functions obtained from FDTD predictions and measurements are displayed.

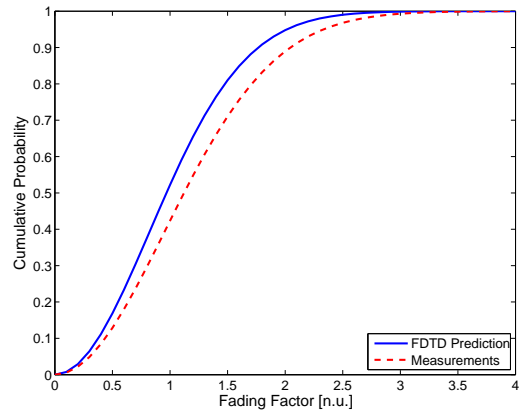


Fig. 5. Cumulative Distribution Function of the Rice distributions extracted both from the FDTD predictions and the real measurements.

TABLE III
RESULTS FOR A PRIVATE ACCESS WiMAX FEMTOCELLS SCENARIO

	No fading	SUI-2	SUI-3	FDTD
Success	82.44%	79.82%	73.12%	78.86%
Cell throughput [Mbps]	2.55	2.44	2.21	2.41

IV. APPLICATION: SIMULATION OF WIRELESS NETWORKS

Fading models are used in system-level simulations to perform realistic predictions of the behavior of wireless communications systems. In a WiMAX system and due to the random attenuation introduced by fading in the OFDMA subcarriers, the packet loss rate of a user may increase. Multipath fading has therefore a direct influence in the overall performance of an OFDMA system.

The fading model presented here has been built into a WiMAX system-level simulator [16] for the evaluation of femtocells environments and matched against the Modified Stanford University Interim (SUI) channel model [17]. The simulated scenario is a residential area with coverage provided by a WiMAX macrocell at $f = 3.5GHz$ and $EIRP = 43dBm$. In addition, indoor WiMAX femtocells with $EIRP = 10dBm$ and omnidirectional antennas are randomly distributed throughout the scenario according to a reasonable forecast of femtocells penetration [18], i.e. approximately 20% of the households containing one femtocell.

Due to its low Doppler effect, the SUI-2 and SUI-3 models can be considered for a first simulation of indoor-to-outdoor femtocells scenarios. As a result of downlink (DL) simulations, Table III indicates the percentage of users able of successfully transmitting their data with certain quality of service (Video) as well as the average achieved cell throughput. It is easy to see that simulations with a fadingless channel overestimate the system performance compared to all other models. The SUI-2 channel model also leads to an overestimation of the global cell throughput and the number of successful users. Meanwhile the SUI-3, which is designed for intermediate path loss conditions, is far more pessimistic due to its lower K factor.

Finally, Figure 6 shows graphically a snapshot of the sce-

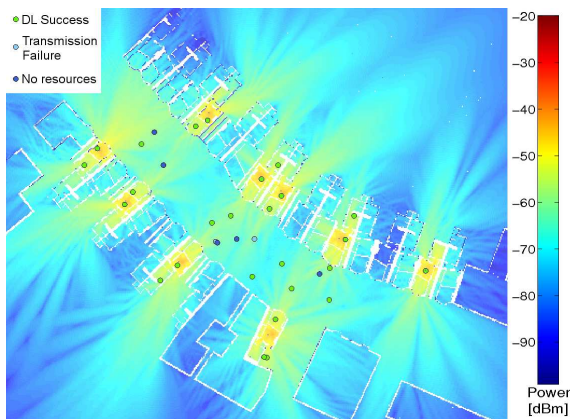


Fig. 6. Random snapshot in a WiMAX system-level simulation containing a distant macro cell and 9 femtocells. The pseudocolor background represents the predicted power received from the best server (either macrocell or femtocell).

nario where the system-level simulations have been performed. It can be seen that some outdoor users suffer occasional outage due to interference from nearby femtocells. This is mainly due to a low SINR in the OFDMA subchannel allocated to the user at an specific time symbol.

V. CONCLUSION

This paper has introduced a deterministic approach for the prediction of small-scale fading distributions in indoor-to-outdoor scenarios. The method has been tested using a calibrated Finite-Difference Time-Domain propagation model, although it is also valid for other Finite-Difference algorithms. Therefore, further research in this area is encouraged.

It has been shown that the characterization of localized random distributions for the modeling of fading in a wireless channel is possible as long as a properly calibrated propagation model is available. The process for the extraction of the fading distribution includes first, an approximation to the coherence distance at the point under consideration and second, a local analysis of the field pattern.

Power measurements have also been collected and used both for the calibration of the FDTD propagation model by means of metaheuristics and for the extraction of the real channel fading statistics. These have been later used for comparison against the FDTD fading distribution predictions.

Finally, the usefulness of this fading predicting approach is tested by means of mobile WiMAX system-level simulations in femtocells scenarios. This is done by comparing the results of the simulations against those thrown when using another existing fading model.

The reliability on the fading distribution is crucial for a careful planning of wireless networks and tiny variations of the simulation results in small areas can lead to vast expenses by part of the network operator. It must be outlined that measurements are an essential part in the calibration process of a radio propagation model and proper measurements campaigns must be performed when developing models for different

telecommunications systems. Thanks to measurements data, the method proposed here can be easily adapted for any frequency, removing thus the need for different fading models, and making it easy for system-level-simulators to predict fading for a wide variety of systems in hybrid indoor/outdoor scenarios.

ACKNOWLEDGMENT

This work is supported by EU FP6 "RANPLAN-HEC" project on 3G/4G Radio Access Network Design under grant number MEST-CT-2005-020958. It is also supported by EU FP6 "GAWIND" project on Grid-enabled Automatic Wireless Network Design with grant number MTKD-CT-2006-042783.

REFERENCES

- [1] G. Mansfield, "Femtocells in the US Market - Business Drivers and Femto cells in the US Market - Business Drivers and Consumer Propositions," in *FemtoCells Europe 2008*. ATT, Jun. 2008.
- [2] A. Taflove and S. C. Hagness, *Computational Electrodynamics: The Finite-Difference Time-Domain Method*, 3rd ed. Artech House, 2005.
- [3] A. Valcarce, G. De La Roche, and J. Zhang, "A GPU approach to FDTD for Radio Coverage Prediction," in *11th IEEE International Conference on Communication Systems*, Nov. 2008.
- [4] G. De La Roche, K. Jaffres-Runse, and J.-M. Gorce, "On predicting indoor wlan coverage with a fast discrete approach," *International Journal of Mobile Network Design and Innovation*, vol. 2, no. 1, pp. 3–12, 2007.
- [5] S. Kirkpatrick, C. D. Gelatt, and M. P. Vecchi, "Optimization by Simulated Annealing," *Science*, vol. 220, no. 4598, pp. 671–680, May 1983.
- [6] A. Valcarce, G. De La Roche, and J. Zhang, "On the use of a lower frequency in finite-difference simulations for urban radio coverage," in *VTC-Spring*, Singapore, May 2008.
- [7] G. De La Roche, X. Gallon, J.-M. Gorce, and G. Villemaud, "On predicting fast fading strength from Indoor 802.11 simulations," in *International Conference on Electromagnetics in Advanced Applications (ICEAA)*, Sep. 2007, pp. 407–410.
- [8] E. Biglieri, R. Calderbank, A. Constantinides, A. Goldsmith, A. Paulraj, and H. V. Poor, *MIMO Wireless Communications*. Cambridge University Press, 2007.
- [9] J.-P. Linnartz. (2006) JPL's Wireless Communication Reference Website. [Online]. Available: <http://wireless.per.nl/reference/contents.htm>
- [10] D. W. Scott, *Multivariate Density Estimation: Theory, Practice, and Visualization*. New York: J. Wiley & Sons Inc., 1992.
- [11] W. Lee and Y. Yeh, "On the estimation of the second-order statistics of log normal fading in mobile radio environment," *IEEE Transactions on Communications*, vol. 22, no. 6, pp. 869–873, Jun. 1974.
- [12] J. L. Rodgers and A. W. Nicewander, "Thirteen ways to look at the correlation coefficient," *The American Statistician*, vol. 42, no. 1, pp. 59–66, 1988. [Online]. Available: <http://dx.doi.org/10.2307/2685263>
- [13] A. Van den Bos, *Handbook of Measurement Science*. Chichester, England: Wiley, 1982, ch. 8, pp. 331–377.
- [14] L. J. Greenstein, S. Ghassemzadeh, V. Erceg, and D. Michelson, "Ricean K-Factors in narrowband fixed wireless channels: Theory, experiments and statistical models," in *WPMC'99 Conference Proceedings*, Sep. 1999.
- [15] A. Abdi, C. Tepedelenlioglu, M. Kaveh, and G. Giannakis, "On the estimation of the K parameter for the Rice fading distribution," *IEEE Communications Letters*, vol. 5, no. 3, pp. 92–94, Mar. 2001.
- [16] D. López-Pérez, A. Valcarce, G. De La Roche, E. Liu, and J. Zhang, "Access Methods to WiMAX Femtocells: A downlink system-level case study," in *11th IEEE International Conference on Communication Systems*, Nov. 2008.
- [17] V. Erceg *et al.*, "Channel Models for Fixed Wireless Applications," IEEE 802.16 Broadband Wireless Access Working Group, Tech. Rep., Jul. 2001.
- [18] ip.access, "Femtocell briefing paper: Introducing 3G femtocells successfully to the home," in *FemtoCells Europe*, 2008.